Published in final edited form as:
Kidney Int. 2011 February ; 79(3): 317–330. doi:10.1038/ki.2010.385.

Dicer regulates the development of nephrogenic and ureteric compartments in the mammalian kidney

Vidya K. Nagalakshmi[1,3], **Qun Ren**[1,3], **Margaret M. Pugh**[1,4], **M. Todd Valerius**[2,5], **Andrew P. McMahon**[2], and **Jing Yu**[1]

[1]Department of Cell Biology, University of Virginia School of Medicine, Charlottesville, Virginia, USA

[2]Department of Stem Cell and Regenerative Biology, Department of Molecular and Cellular Biology, Harvard Stem Cell Institute, Harvard University, Cambridge, Massachusetts, USA

Abstract

MicroRNAs (miRNAs) are a large and growing class of small, non-coding, regulatory RNAs that control gene expression predominantly at the post-transcriptional level. The production of most functional miRNAs depends on the enzymatic activity of *Dicer*, an RNase III class enzyme. To address the potential action of *Dicer*-dependent miRNAs in mammalian kidney development, we conditionally ablated *Dicer* function within cells of nephron lineage and the ureteric bud-derived collecting duct system. *Six2Cre*-mediated removal of *Dicer* activity from the progenitors of the nephron epithelium led to elevated apoptosis and premature termination of nephrogenesis. Thus, *Dicer* action is important for maintaining the viability of this critical self-renewing progenitor pool and, consequently, development of a normal nephron complement. *HoxB7Cre*-mediated removal of *Dicer* function from the ureteric bud epithelium led to the development of renal cysts. This was preceded by excessive cell proliferation and apoptosis, and accompanied by disrupted ciliogenesis within the ureteric bud epithelium. *Dicer* removal also disrupted branching morphogenesis with the phenotype correlating with downregulation of *Wnt11* and *c-Ret* expression at ureteric tips. Thus *Dicer*, and by inference *Dicer*-dependent miRNA activity, have distinct regulatory roles within different components of the developing mouse kidney. Furthermore, an understanding of miRNA action may provide new insights into the etiology and pathogenesis of renal cyst-based kidney disease.

Keywords

branching morphogenesis; *Dicer*; miRNA; nephron progenitors; primary cilium; renal cyst

MicroRNAs (miRNAs) are a large and growing class of small, non-coding, regulatory RNAs that control gene expression predominantly at the post-transcriptional level through direct binding to target mRNAs. In general, miRNAs function by inhibiting protein

Correspondence: Jing Yu, Department of Cell Biology, University of Virginia School of Medicine, 1340 Jefferson Park Avenue, Charlottesville, Virginia 22908, USA. jy4m@virginia.edu.

[3]These authors contributed equally to this work.

[4]Current address: Diffusion Pharmaceuticals LLC, Charlottesville, Virginia, USA.
[5]Current address: Transplant Institute, Beth Israel Deaconess Medical Center, Boston, Massachusetts, USA.

DISCLOSURE

All the authors declared no competing interests.

Supplementary material is linked to the online version of the paper at http://www.nature.com/ki

translation and/or degrading target mRNAs (for recent reviews, see Carthew and Sontheimer[1]; Behm-Ansmant *et al*.[2]; Pillai *et al.*[3]), although recent reports indicate that miRNAs may occasionally enhance expression from their target mRNAs in a tissue context- or cell cycle state-dependent fashion.[4,5] A single miRNA may regulate hundreds of target genes, and a given gene can be regulated by multiple miRNAs. In this way, miRNA action underpins many fundamental biological processes, including developmental timing, apoptosis, cell proliferation, cell-fate choice and morphogenesis, as well as pathogenic cellular activities, notably oncogenesis.[6]

miRNAs are initially transcribed as long pri-miRNAs from miRNA-coding genes and need to be processed to function. *Dicer*, an RNase III class enzyme, is required for the processing of most miRNAs. pri-miRNAs are first processed in the nucleus by another RNase III, Drosha, in a complex with DGCR8, or the splicing machinery, to ~70 nt stem-loop pre-miRNAs. *Dicer* then processes pre-miRNAs in the cytoplasm to mature miRNAs, which recognize cognate mRNAs through an Argonaute-dependent process, modulating the stability or translation of mRNA targets (see Carthew and Sontheimer[1] for a recent review). Genetic studies with conditionally removing *Dicer* function have demonstrated critical roles for *Dicer*-mediated miRNA regulation in the development and function of a variety of mammalian tissues and organs.[7,8]

Kidney development is driven by reciprocal interactions between the ureteric bud (UB) epithelium and the overlying metanephric mesenchyme (for a recent review, see Dressler[9]), with additional inputs from the renal interstitium and vascular tissues.[10–16] The UB epithelium originates as an evagination of the Wolffian duct epithelium at the hind-limb level.[17] UB-derived signals regulate maintenance and nephron commitment within a *Six2*+ mesenchymal progenitor compartment that caps the branching ureteric tips (nephron progenitors).[18–20] Inductive UB signals induce a mesenchymal-to-epithelial transition within overlying progenitor pools, resulting in the emergence of the renal vesicle beneath the UB tip.[19] The renal vesicle is the nephron precursor, and its morphogenesis, patterning, and differentiation establishes the mature renal tubular, visceral, and parietal epithelia of the nephron. Metanephric mesenchyme-secreted Glial cell line-derived neurotrophic factor (GDNF) stimulates branching morphogenesis of the subjacent UB tips, establishing the highly branched network of the renal collecting duct system (recently reviewed in Costantini[17]). Epithelial growth within both nephron and collecting duct epithelia is tightly controlled; deregulation leads to cystic dilation and renal cystic diseases. Through these intricate interactions, the UB branching morphogenesis regulates nephron numbers, a predisposing factor for renal diseases and hypertension.[21,22]

Evidence for the involvement of *Dicer* and miRNAs in kidney development and homeostasis is accumulating.[23–25] miRNAs have been detected in embryonic and adult kidney tissues and changes in miRNA expression have been observed in various kidney diseases, including polycystic kidney disease, diabetic nephropathy, kidney and bladder cancer, and in autoimmune disease like lupus nephritis.[23–25] Podocyte-specific removal of *Dicer* causes multiple abnormalities in postnatal renal corpuscle homeostasis and function, leading to proteinuria and a rapid progression to end-stage kidney diseases.[26–28] Maintenance of Juxtaglomerular cells also requires *Dicer* input.[29] Removal of *Dicer* within the collecting duct epithelium results in postnatal hydronephrosis and collecting duct cysts,[30] demonstrating the functional importance of *Dicer* and miRNAs in kidney homeostasis and function. In addition, miRNAs regulate *Xenopus* pronephros patterning and differentiation.[31]

In this paper, we use nephron progenitor-specific *Dicer* removal to demonstrate the importance of *Dicer* in the maintenance of nephron progenitors and nephron epithelia.

Conditional removal of *Dicer* within the adjacent ureteric bud epithelium extends a previous report[30] of *Dicer*/miRNA-associated cystic dilation by identifying a requirement for *Dicer* in controlling cell proliferation and apoptosis in the collecting duct epithelium. Furthermore, we demonstrate that *Dicer* action is required for normal branching growth of the ureteric network.

RESULTS

Removal of *Dicer* activity from the nephron lineage leads to premature depletion of nephron progenitors

To examine the overall involvement of nephron lineage-expressed *Dicer* and miRNAs in kidney development, we ablated *Dicer* function from the entire nephron lineage using a *Six2Cre* (*Six2TGC*) transgenic mouse strain.[18] The resulting mutant mice (*Dicer*$^{c/-}$*; Six2TGC*, referred to as *Dicer* nephron mutants hereafter) died within 36h post-partum. Examination of expression of randomly selected mature miRNAs with miRNA *in situ* hybridization and semiquantitative reverse transcription-PCR analyses suggests that miRNA maturation was specifically disrupted in the nephron lineage in the mutant kidneys (Figure 1a).

The mutant newborn kidneys were smaller than the control littermates, with a striking 93.2% reduction in nephron numbers (control, 1755; mutant, 119; P<3.1E-12, n = 7) (Figure 2 and Supplementary Figure S1A online). Moreover, the nephron progenitors and developing nephron structures (renal vesicle, comma-shaped body, and S-shaped body) were absent from many regions of the renal cortex (Figure 2e and f). Consistent with the latter observation, *Six2* expression in the nephron progenitors was lost in many areas of the mutant kidney cortex (Figure 3b). Notably, in regions where the nephrogenic zone was still present, there were much fewer nephron progenitor cells capping the UB tips (Pax2+ cap mesenchyme cells) (Figure 3a). Moreover, most of these mutant nephron progenitor cells expressed green fluorescent protein (GFP; as a fusion protein with Cre) at greatly reduced to undetectable levels, in contrast to the strong expression of GFP in all cells of their control counterparts (Figure 3a). The *Six2TGC* driver line was generated by BAC (bacterial artificial chromosome) transgenics in that a large fragment of the genomic sequence encoding the endogenous *Six2* promoter drives the expression of the GFP/Cre fusion protein. The reduction in GFP levels in *Dicer* mutant nephron progenitors may reflect downregulation of the activity of the *Six2* promoter driving GFP/Cre expression. If this is the case, the expression of endogenous *Six2* gene should also be compromised in *Dicer* nephron mutants. Indeed, we observed a decrease in the levels of *Six2* transcripts, where present, in mutant nephron progenitors (Figure 3b, insets). Taken together, these data suggest that *Dicer* and presumably miRNAs are critical for the maintenance of nephron progenitors and *Six2* expression.

Quantitative analysis showed that the reduction in the number of nephron progenitor cells (Pax2+ cap mesenchyme cells) per ureteric tip was first evident at embryonic day (E)15.5 (Figure 3c). The reduction in GFP expression in nephron progenitors was observed in a subset of cells as early as E13.5 (Figure 3a), preceding the onset of the premature loss of nephron progenitors, and exacerbated later in development (Figure 3a and d, the percentage of GFP+ nephron progenitors: 82.3% at E14.5, 73.2% at E15.5). Likewise, *Six2* transcript levels were reduced prior to the onset of the premature loss of nephron progenitors (Figure 3b).

Dicer regulates nephron progenitor cell survival

To determine the cellular mechanisms underlying the premature depletion of nephron progenitor cells following *Dicer* removal, we examined cell proliferation, cell survival, and cell differentiation at E14.5, prior to the observed phenotype. Cell proliferation, as determined by 5-bromo-deoxyuridine (BrdU) incorporation, was unaffected (data not shown). The earliest markers of nephron induction, *Wnt4* and *Fgf8*, were expressed in the normal pattern underneath the UB tips, and not in mutant nephron progenitors overlying the ureteric tips (Supplementary Figure S2A online), ruling out precocious differentiation of nephron progenitors. Moreover, cell-fate mapping with a *Rosa26lacZ* Cre reporter[32] in the *Dicer* nephron mutant background showed that mutant nephron progenitors only contributed to the nephron lineage and did not trans-differentiate into other renal cell types (Supplementary Figure S1B online). In contrast, when apoptosis in the Pax2+ cap mesenchyme cells was examined with TUNEL (TdT-mediated dUTP nick end labeling) analysis, an increase in apoptosis in the mutant nephron progenitors was readily observed (Figure 4a). In the control kidneys, apoptotic cells were rarely seen in nephron progenitors (1.24±0.94%, $n = 3$), whereas in the mutants the apoptosis rate increased by almost six-fold to 7.27±2.59% ($n = 4$). Taken together, these data demonstrate that *Dicer* action is important for survival of nephron progenitors.

Increased apoptosis in the nephron epithelium

Disruption of *Dicer* function did not appear to affect nephron patterning, as judged by the normal expression patterns of markers for different segments of the S-shaped bodies, *Wt1* (proximal segment), *Wnt4* (medial segment), *Fgf8* (medial segment), and *Brn1* (medial and distal segments) in *Dicer* nephron mutants (Supplementary Figure S2B). Moreover, nephron segmentation and terminal differentiation was also largely normal at E15.5, based on the expression of nephron segmentation and differentiation markers (Supplementary Figure S3 online).

Although most of segmentation and differentiation markers were expressed at normal levels at the early stage of nephron segmentation and terminal differentiation, the expression level of *Gsh1*, one of the earliest markers of the podocyte lineage, was greatly reduced in mutant kidneys (Supplementary Figure S3 online). To determine whether reduced *Gsh1* expression reflected global disruption of podocyte differentiation, we examined the expression of two additional podocyte markers, WT1 and p57Kip2. The expression of neither gene in mutant podocytes was obviously altered (Supplementary Figure S3 online), suggesting that *Gsh1* expression was specifically affected by *Dicer* removal.

Although cell differentiation was undisturbed in mutant nephrons, cell death was markedly elevated in the proximal segment of the S-shaped body and the Cadherin 6+ nephron tubules (Figure 4b), indicating an extended role for *Dicer* action in cell survival within the developing nephron epithelium.

Premature termination of branching morphogenesis in *Dicer* UB mutant kidneys

Dicer was specifically ablated from the UB epithelium with a *HoxB7Cre* deletor line; Cre recombinase driven by a *Hoxb7* promoter is specifically expressed throughout the Wolffian duct from E9.5, prior to the outgrowth of the ureteric bud, and high levels of expression are maintained within all UB derivatives after kidney development initiates.[33] The resultant mutants (*Dicer*$^{c/-}$*; HoxB7Cre)* died by 24–48h post-partum, suggesting that *Dicer* in the UB epithelium is essential for kidney development. This is in contrast to viable *HoxB7*$^{Cre/+}$*; Dicer1*$^{flox/flox}$ mice reported by Pastotelli *et al.*[30] The discrepancy in viability probably reflects decreased efficiency in Cre-mediated deletion of *Dicer*, where both alleles are conditional null that may lead to higher frequency of mosaic removal, an observation that

accounts for variability in *Dicer* mutant phenotypes in podocytes.[27] In a second genetic cross, we removed *Dicer* activity with a *HoxB7Cre-Ires-EGFP* line (*HoxB7CreEGFP* for short).[34] Here, analysis of enhanced GFP (EGFP) activity suggests variable levels of Cre expression (data not shown). Remarkably, most $Dicer^{c/-}$*; HoxB7-CreEGFP* survived to adulthood (Figure 5j, and data not shown) and exhibited hydronephrosis and hydroureter as observed in $HoxB7^{Cre/+}$*;* $Dicer1^{flox/flox}$ mice. In some hydronephrotic mutant kidneys, only a thin layer of the renal cortex remained, whereas some mutants with milder phenotypes retained most of the renal parenchyma but developed cysts in the collecting ducts (Figure 5j and data not shown), similar to $HoxB7^{Cre/+}$*;* $Dicer1^{flox/flox}$ kidneys.[30]

As $Dicer^{c/-}$*; HoxB7Cre* mice exhibited a more consistent, severe phenotype distinct from that reported earlier, subsequent studies focused on this genotype (referred to as *Dicer* UB mutants hereafter). As the kidneys of *Dicer* heterozygotes including $Dicer^{c/+}$*; HoxB7Cre* littermates retaining one active *Dicer* allele appeared normal, these samples were pooled with wild-type littermates for controls.

Examination of randomly selected miRNAs showed that expression of mature miRNAs in the UB epithelium of *Dicer* UB mutants was greatly reduced to near-undetectable levels, whereas their expression in the non-UB epithelial components of the kidneys was unaffected (Figure 1), suggesting that ablation of *Dicer* from the UB epithelium disrupted mature miRNA expression specifically in this cell population.

A gross examination of *Dicer* UB mutant kidneys at P0 indicated that kidneys were markedly smaller than those of wild-type littermates (Figure 5). In contrast to the wild-type kidney at P0, where branching ureteric tips uniformly distributed about the periphery of the renal cortex, the renal cortex was (mostly) devoid of branching tips in *Dicer* UB mutants (Figure 5). Consistent with the histological observation, *in situ* hybridization to P0 *Dicer* UB mutants revealed a complete absence of expression of *Wnt11* (Figure 5i and j) or c-Ret (Supplementary Figure S4 online), the two critical regulators of normal UB branching, in the periphery of most mutant kidneys. Furthermore, pan-Cytokeratin staining of whole-mount E15.5 kidneys showed a drastic reduction of the ureteric bud network (Supplementary Figure S4). Thus, *Dicer* activity is essential for protracted branching of the UB epithelium, with loss of *Dicer* resulting in a premature termination of branching morphogenesis.

Reduced expression of *Wnt11* and *c-Ret*, but not *GDNF*, at the onset of branching defects in *Dicer* UB mutants

Quantitative measurements showed that *Dicer* UB mutant kidneys were of similar size to the controls at E13.5 ($P<0.43$, $n = 3$), but were 21.8% smaller than their controls at E14.5 ($P<0.04$, $n = 3$, and Supplementary Figure S5 online), suggesting that defects in branching morphogenesis occurred shortly before E14.5. We thus examined branching morphogenesis at E13.5 to investigate the molecular causes for the branching defect. *In situ* analysis on whole-mount E13.5 kidneys revealed a dramatic reduction in the number of *Wnt11*-positive tips and in the levels of *Wnt11* expression in *Dicer* UB mutants (Figure 6a and b). To differentiate whether the decreased number of *Wnt11*-positive tips is because of a reduced number of ureteric tips or the lack of *Wnt11* expression in a subset of ureteric tips, we performed double *in situ* hybridization analysis on E13.5 kidney sections (Figure 6) to simultaneously detect *Wnt11* at the UB tips (brown) and mark the UB trunks with *Wnt7b* expression (purple). Examination of all ureteric branches in tissue sections spanning entire kidneys clearly demonstrated that all mutant tips expressed *Wnt11*, although at reduced levels.

GDNF is the major stimulatory factor for UB branching morphogenesis and *Gdnf/Ret* signaling is itself required for *Wnt11* expression at ureteric tips.[35] To determine whether

reduced *Wnt11* expression at E13.5 resulted from decreased *Gdnf* expression, we examined *Gdnf* mRNA expression at E13.5 (Figure 6). *Gdnf* expression appeared normal in *Dicer* UB mutants. The results indicate that the primary deficiency in *Wnt11* expression appears to lie within the UB epithelium and not indirectly from reduced GDNF levels in the mesenchyme. Consistent with a role for *Dicer* in controlling the epithelial branching circuitry, expression of *c-Ret*, the *Gdnf* receptor, was also markedly reduced within the ureteric tips, and most likely as a result, reception of the branching signal was decreased (Figure 6j).

Defects in cell proliferation and apoptosis underlie cyst formation in *Dicer* UB mutants

Consistent with and extended from the study by Pastorelli *et al*.,[30] which reported cortical collecting duct cysts in mutant mice at ≥3 weeks of age, our histological examination revealed the presence of cysts throughout the UB epithelium in *Dicer* UB mutant kidneys at P0 (Figure 5), which were first apparent at around E15.5 (Supplementary Figure S5 online) in the nascent trunk region adjacent to the ureteric tips (Figure 5, Supplementary Figure S6A online). More enlarged cysts were detected in $Dicer^{c/-}$*; HoxB7CreEGFP* mice (Figure 5l) (cyst area, 20.2±14.0 × 10^3 μm^2 in $Dicer^{c/-}$*; HoxB7CreEGFP* p38 kidneys; 2.4±1.3 × 10^3 μm^2 in $Dicer^{c/-}$*; HoxB7Cre* P0 kidneys, n = 25, P<1.4E-06), probably because the longer survival time allows for more extended cyst progression.

Overproliferation precedes and accompanies renal cyst initiation and progression in most polycystic kidney disease models.[36–39] To dissect for the cellular causes for cyst formation in *Dicer* UB mutants, we quantified the cell proliferation rate in the nascent ureteric trunk region at E14.5 and cystic UBs at E15.5 by BrdU incorporation. A significantly elevated rate of cell proliferation was observed in mutant UB epithelia both before and after the initiation of cystic dilation when compared with their control counterparts (Figure 7a). Thus, excessive cell proliferation is probably a major contributing factor for both the onset and acceleration of cystic phenotypes in *Dicer*-deficient UB epithelium.

Another common feature associated with renal cysts is increased apoptotic cell death.[40–42] We examined the rate of apoptosis in *Dicer* mutants with TUNEL analysis. No statistically significant differences were observed in the rate of cell death between the mutants and the controls at E14.5 (data not shown). In contrast, apoptosis was markedly increased in the non-dilated UB epithelium shortly before the onset of cyst formation (E15.25) and in cystic UB epithelium at E15.5 (Figure 7b). Thus, enhanced apoptosis correlates with both the initiation and progression of cyst formation.

Disruption of primary cilial ciliogenesis at the onset of cyst formation in the *Dicer* UB mutant UB epithelium

The primary cilium is a central organelle in cyst formation.[43] Disruption of ciliogenesis (the absence of or runted primary cilia) results in cystic kidneys. Strikingly, we observed a significant decrease in the length of the primary cilium in ureteric trunks just initiating cystic dilation (dilating UBs) as well as in well-expanded cysts (cystic UBs) at E15.5 (Figure 8). In all, 42% of primary cilia were >4 μm in length and only 4.8% of them were <2 μm in control UBs. In contrast, only 2.5 and 6.8% of primary cilia were >4 μm, and 41.3 and 37.1% of them <2 μm in dilating and cystic mutant UBs, respectively. The defect in primary cilia length was specific to the UB epithelium, as no significant differences were observed between mutant and control littermates in other renal cell types (Supplementary Figure S6B online).

In contrast, at E14.5 and in non-dilating UBs at E15.25 (right before the cyst onset), there was no detectable difference in the primary cilia length between the wild-type and mutant ureteric trunks (Figure 8, and data not shown). Interestingly, we noticed that even in the wild

type, the primary cilia in the E14.5 and E15.25 nascent ureteric trunk region were shorter than those at E15.5 (Figure 8), suggesting that the primary cilium normally elongates between E15.25 and E15.5. Therefore, the primary cilia defects in dilating and cystic UBs of Dicer UB mutants either reflect a consequence of cystic dilation, or a disruption of this developmental switch of primary cilia elongation. We also cannot rule out the possibility of precocious activation or acceleration of primary cilium disassembly during each cell cycle starting at E15.5 due to *Dicer* deficiency.

Terminal differentiation of the ureteric bud epithelium appears defective in *Dicer* UB mutants

To investigate terminal differentiation of the UB epithelium in *Dicer* UB mutants at P0, we examined the expression of *Foxi1* and *Aqp6*, the markers for early and late differentiation of intercalated cells, and *Nos1*, a marker of the inner medullary collecting duct cells. *Aqp6* and *Nos1* were expressed at lower levels and/or at a reduced frequency in the mutant epithelium (Figure 9), whereas the *Foxi1* expression pattern was unaltered. The disrupted expression of *Aqp6* and *Nos1* was not because of apoptosis of the collecting duct cells (Supplementary Figure S7 online). These results suggest that collecting duct differentiation was initiated normally but terminal differentiation was disturbed on removal of *Dicer* activity from the UB epithelium.

DISCUSSION

We have addressed the requirement for *Dicer* activity within the nephron lineage (nephron progenitors and nephron epithelia) and the epithelial network of the developing renal collecting duct system, the major functional components of the kidney. The study reveals a critical role for *Dicer* in survival of the nephron lineage, including the stem-like nephron progenitors and the nephron epithelium, and normal branching, radial growth, and terminal differentiation of the ureteric bud epithelium. Our findings confirmed a previous report of cyst formation in the absence of *Dicer* functions and pointed to increased cell proliferation and apoptosis and disruption of ciliogenesis in the etiology and pathogenesis of cyst formation in the *Dicer* UB knockout model. Given *Dicer*'s critical function in the maturation of most miRNAs in mammalian cells, our work implicates *Dicer*-dependent miRNA-mediated regulation in the control of nephron number and epithelial growth and survival, properties that are linked to a variety of renal diseases.[44]

Maintenance of nephron progenitors by *Dicer*

Dicer-deficient nephron progenitors underwent premature apoptosis. How *Dicer* and miRNAs are involved in the regulation of the survival of nephron progenitors is unclear at present. The transforming growth factor-β superfamily signaling has been shown to be involved in the maintenance of nephron progenitors.[45] However, this superfamily signaling appears to regulate the organization/recruitment of nephron progenitors. In the absence of this signaling, these cells failed to condense, and are instead loosely associated and embedded in the renal interstitium.[45] This phenotype is distinct from ablation of *Dicer* from nephron progenitors, in which nephron progenitors were tightly condensed over the ureteric tips and not intermingled with interstitial cells. Furthermore, recent studies showed that *Bmp7* acts to promote proliferation of nephron progenitors.[46] Taken together, this suggests that *Dicer* and miRNAs do not modulate nephron progenitor survival through transforming growth factor-β superfamily signaling.

Six2 mRNA levels were reduced in *Dicer* mutant nephron progenitor cells. Notably, it was previously reported that *Six2*-null nephron progenitors exhibited increased apoptosis,[20] and decreased expression of *Six2* was associated with low nephron numbers and small

embryonic and adult kidney size in Brachyrrhine (*Br/+*) mice.[47,48] It is possible that reduced levels of expression of *Six2* contribute to the increase in apoptosis of nephron progenitors resulting from *Dicer* ablation.

Branching defects in *Dicer* UB mutants

Elimination of *Dicer* from the UB epithelium causes UB branching defects. Interestingly, ablation of *Dicer* from lungs also produced branching deficiencies,[49] suggesting a principal function of *Dicer* and presumably of miRNAs in regulating epithelial branching morphogenesis, one of the most common developmental processes driving epithelial organ formation. On the other hand, the mechanisms whereby *Dicer* and miRNAs regulate branching morphogenesis appear organ specific. In lungs, epithelial miRNAs appear to modulate branching morphogenesis in a paracrine fashion by regulating the production of the lung branching signal, *Fgf10*, in the mesenchyme. In contrast, in the kidney, we found that at an early developmental time point when the branching defect begins to manifest and the expression of *Wnt11* and *c-ret*, the two molecules in ureteric tips required for proper UB branching, was greatly reduced, the expression of the major UB branching signal in the mesenchyme, *Gdnf*, was not obviously affected. Therefore, in the kidney, unlike the lungs, *Dicer* in the UB epithelium appears to regulate the reception of branching signals and the execution of branching morphogenesis in the UB epithelium, instead of the production of the branching signal in the mesenchyme.

Wnt11 and *Gdnf*/*c-Ret* signaling form a positive feedback loop.[35] It is possible that reduced expression of *Wnt11* resulted from reduced *Gdnf*/*c-Ret* signaling because of decreased expression of *c-Ret*.

Molecular and cellular mechanisms underlying the cystic defects in *Dicer* UB mutants

Cysts were observed starting from E15.5 in the collecting duct system in our *Dicer* UB mutant mouse model. A recent study from Pastorelli *et al.*[30] also reported the cystic phenotype at postnatal stages from removal of *Dicer* function with HoxB7Cre. These studies demonstrated the importance of *Dicer* and presumably miRNAs in UB epithelium tube size control. Our analysis showed that UB-specific *Dicer* and miRNAs are involved in the regulation of cell proliferation and apoptosis in UB cells. Elevated cell proliferation and apoptosis rates precede and accompany cyst onset and progression, arguing strongly for their causal link with the UB cystic defect.

Cystic renal disease is a ciliopathy.[43] Runted primary cilia were observed in cystic renal epithelial cells of *orpk* (oak ridge polycystic kidney) mice,[50] which bear a hypomorphic insertional mutation in *Ift88* (*Polaris*),[51,52] an intraflagellar transporter gene that is required for ciliogenesis.[50,53] Notably, the primary cilia were severely shortened in the UB epithelium just initiating cystic dilation (dilating UBs) and in cystic UBs in *Dicer* UB mutants, but not in the UB epithelium before the cyst onset. However, the primary cilium of control kidneys is equally short as those of the mutants before the cyst onset, but increases dramatically in length at the developmental time point when cysts start to form in *Dicer* UB mutants. Taken together, this suggests that defects in ciliogenesis in *Dicer* UB mutants could result from either a disruption of this developmental switch of primary cilia elongation, or cystic dilation.

In proliferating cells, the primary cilium disassembles to release the centrioles (basal body) at each cell cycle for cell division.[54] Therefore, the distribution of the primary cilium length within a population of proliferating cells may be affected by their proliferation rate. However, it seems less likely that the primary cilia phenotype observed in E15.5 *Dicer* UB

mutant cells is secondary to their cell proliferation defect, as the primary cilium length in E14.5 *Dicer* mutant UB cells, which are also hyperproliferative, is unaffected.

Our analysis of global functions of UB and nephron lineage-derived *Dicer* identified key kidney developmental events that require the inputs from *Dicer* and presumably miRNAs. This defines the scope of involvements of nephron lineage- and UB-specific *Dicer* and presumably miRNAs in kidney organogenesis; moreover, it provides functional readouts for future analysis of individual miRNAs and their targets implicated in these processes. Experimental manipulation of individual miRNA expression has proved that a single miRNA regulates the expression of hundreds of targets, many of them only to a modest degree.[55–57] Likewise, individual developmental defect resulted from *Dicer* ablation is likely to be a collective effect from disruption of multiple miRNAs and a large number of their target genes. A genomic approach is therefore necessary and is under way to identify these miRNAs and their target genes/pathways for future functional analysis of individual miRNAs and targets toward full appreciation of the molecular mechanisms underlying each of the renal developmental processes in the nephron lineages and the UB epithelium mediated by *Dicer* and miRNA functions.

MATERIALS AND METHODS

Mice

The conditional *Dicer* allele (*Dicer*^{c}) was previously described.[58] The *Dicer*$^{-}$ allele was generated from the *Dicer*^{c} allele with a *Sox2Cre*.[59] The *Six2TGC* driver mouse, a BAC transgenic line, was described in Kobayashi *et al*.[18] The HoxB7Cre and HoxB7CreEGFP mice were previously described.[33,34] Animal experiments were performed in accordance with the policies of the institutional animal care and use committee at the University of Virginia.

Tissue preparation

Tissue preparation for histological staining on paraffin sections, immunofluorescent staining, and *in situ* hybridization on cryosections were done as described in Yu *et al*.[60] For scanning electron microscopy, freshly dissected mouse embryonic kidneys were fixed with 2.5% glutaraldehyde in phosphate-buffered saline (PBS) at 4 °C overnight and embedded in optimal cutting temperature. For BrdU labeling, pregnant female mice were injected intraperitoneally with 0.5 mg BrdU per 10 g body weight at 2h before the harvest of embryonic kidneys. For whole-mount *in situ* hybridization, kidneys were fixed with 4% paraformaldehyde in PBS at 4 °C for 24h, washed with PBS, and dehydrated with a graded series of methanol/0.85% NaCl solutions and stored in 100% methanol at −20 °C.

Histology, immunostaining, and quantification

Paraffin blocks were sectioned at 5 to 6 μm for hematoxylin and eosin staining as previously described.[33] Nephron numbers were quantified by counting renal corpuscles in hematoxylin and eosin-stained sections. The kidney size (the pole-to-pole length) was measured from histological sections at the central-most plane. Frozen blocks were sectioned at 12 μm for immunostaining using a standard protocol.[60] For co-staining with two primary antibodies made from the same host species, one of the antibodies was labeled with Zenon labeling technology (Invitrogen, Carlsbad, CA) following the manufacturer's instructions. TUNEL staining was performed with the ApopTag Red *In situ* Apoptosis Detection Kit (Chemicon International, Billerica, MA), following the manufacturer's instruction. Immunostained images were visualized using a Personal Deltavision microscope (Applied Precision, Issaquah, WA) and collected with a digital camera (Photometrix, CoolSNAP *HQ*^{2}, Tucson, AZ). For quantification of cell proliferation and apoptosis rates, 200–400 cells were counted

in 2 to 3 kidney sections per embryo, from 3 to 4 embryos. Primary antibodies used in this study were as follows: anti-Pax2 (Covance, Princeton, NJ; 1:500); anti-Laminin (Sigma, St Louis, MO; 1:2000); anti-GFP (Aves Labs, Tigard, OR; 1:500); anti-β-galactosidase (Abcam, Cambridge, MA; 1:1500); anti-β-galactosidase (MP Biomedicals, Solon, OH; 1:10,000); anti-pan-Cytokeratin (Sigma; 1:200); *Dolichos bifloris* agglutinin (DBA)-Biotin (Sigma; 1:500); anti-BrdU (BD Pharmingen, San Diego, CA; 1:100); anti-WT1 (Santa Cruz Biotechnology, Santa Cruz, CA; 1:50); and anti-Cdh6 (gifts of Dr Dressler; 1:100).

lacZ staining

Freshly dissected kidneys from the mice were fixed in 2% paraformaldehyde at 4 °C for 1h and embedded in optimal cutting temperature. Frozen blocks were sectioned at 12 μm and stained in *lacZ* staining solution at 4 °C overnight.[33]

In situ hybridization

In situ hybridization analysis was performed on whole-mount kidneys (whole-mount *in situ* hybridization) as well as on sections from frozen blocks (section *in situ* hybridization). Frozen blocks were sectioned at a thickness of 16 μm for single and double *in situ* hybridizations and 30 μm for some of the double *in situ* hybridizations. Section *in situ* hybridization was performed essentially the same as in Yu *et al*.[33,60] For double *in situ* hybridization, tissue sections were hybridized with a mixture of digoxigenin- and fluorescein-labeled riboprobes, each at the concentration of 500 ng/ml. After detection of digoxigenin-labeled probe, sections were fixed and then incubated with anti-fluorescein-alkaline phosphatase antibody (1:2000; Roche, Indianapolis, IN) at 4 °C overnight. Signals were developed using INT/BCIP dissolved in 10% polyvinyl alcohol.

Detection of miRNAs with *in situ* hybridization on kidney frozen sections was performed similarly except that tissue sections were hybridized with 25 nM digoxigenin-labeled locked nucleic acid probes. Kidney sections were not treated with RNase A after hybridization. Hybridization and post-hybridization washes were performed at 60 °C.

For whole-mount *in situ* hybridization, kidney samples were rehydrated with a graded series of methanol/0.85% NaCl, treated with 10 μg/ml Proteinase K for 10 min, and prehybridized in pre-hybridization buffer (50% formamide, 5 × SSC, pH 4.5, 50 μg/ml yeast tRNA, 1% SDS, and 50 μg/ml heparin) before hybridization at 70 °C. Post-hybridization washes were performed at 65 °C before treatment with 100 μg/ml RNase at 37 °C for 1h. Samples were then incubated with anti-digoxigenin-alkaline phosphatase at 4 °C overnight. Signals were detected with BM purple. After being post-fixed with 4% paraformaldehyde/0.1% glutaraldehyde, samples were cleared with a graded series of glycerol/PBS and stored in 80% glycerol/PBS at 4 °C. Images were collected with a Leica MZ16F stereoscope equipped with a DFC300 FX camera (Leica Micro Systems, Bannockburn, IL).

Electron microscopy

Sections were cut at 150 μm thickness and fixed further for 20 min in 2.5% gluteraldehyde. Sections were processed following a standard protocol.[61] Samples were sputter coated with 30 nm of gold in sputter coater (BAL-TEC SCD005; Leica Micro Systems, Bannock-burn, IL) and observed on a scanning electron microscope (JEOL 6400; JEOL, Peabody, MA). The primary cilia length was measured using the ImageJ software (1.37b; National Institutes of Health, Bethesda, MD) from three to four mutant as well as control embryos.

RNA purification, reverse transcription, and quantitative or semiquantitative PCR

Total RNA was purified from E13.5 kidneys with RNeasy mini kit (Qiagen, Valencia, CA), and reverse transcribed with random hexamers with a Tetro cDNA synthesis kit (Bioline,

Taunton, MA). Quantitative PCR on *Six2* and *β-actin* was performed with SYBR Green JumpStart Taq ReadyMix (Sigma) on DNA Engine Chromo 4 (Bio-Rad, Hercules, CA). *Six2* transcript levels were normalized with that of *β-actin*. Oligonucleotide primers used for PCR were: Six2RTs: 5′-GAAAGGGAGAACAGCGAGAA-3′, Six2R-Tas: 5′-CTTCTCATCCTCGGAACTGC-3′, *β*-actin fwd: 5′-GATC TGGCACCACACCTTCT-3′, *β*-actin rev: 5′-GGGGTGTTGAAGGTCTCAAA-3′.

GFP-positive cap mesenchyme cells (nephron progenitors) were sorted from E13.5 *Dicer*$^{c/-}$*; Six2TGC* and *Dicer*$^{c/+}$*; Six2TGC* (control) kidneys with a Becton Dickinson FACSVantage SE Turbo Sorter with DIVA Option (BD Biosciences, San Jose, CA). Total RNAs including miRNAs and mRNAs were purified from sorted cells with the miRNeasy mini kit (Qiagen), and reverse transcribed with the miScript PCR system (Qiagen), which reverse transcribes miRNAs and mRNAs in the same reaction. Semiquantitative PCRs for mature mmu-miR-30a, mmu-miR-30b, and mmu-miR-30c were performed with the miScript PCR system (Qiagen), using the miScript Primer Assays (Qiagen) for each mature miRNAs, for 29, 31, and 29 cycles, respectively. Semiquantitative PCR for *β-actin* was performed with SYBR Green JumpStart Taq ReadyMix (Sigma) for 25 cycles.

Statistical analysis

Statistical significance was determined using Student's *t*-test.

Supplementary Material

Refer to Web version on PubMed Central for supplementary material.

Acknowledgments

We thank Michael McManus, Brian Harfe, and Cliff Tabin for providing the *Dicer*$^{c/c}$ mice, Calton Bates for the HoxB7CreEGFP mice, Gregory Dressler for anti-Cadherin 6 antibodies, and Jan Redick at the University of Virginia Advanced Microscopy Facility for technical assistance in scanning electron microscopy. Work in the laboratory of APM was supported by a grant from the NIH (DK054364). Work in the laboratory of JY was supported by a UVA Fund for Excellence in Science and Technology (FEST) Award, and research grant 5-FY09-102 from the March of Dimes Foundation.

References

1. Carthew RW, Sontheimer EJ. Origins and mechanisms of miRNAs and siRNAs. Cell. 2009; 136:642–655. [PubMed: 19239886]
2. Behm-Ansmant I, Rehwinkel J, Izaurralde E. MicroRNAs silence gene expression by repressing protein expression and/or by promoting mRNA decay. Cold Spring Harb Symp Quant Biol. 2006; 71:523–530. [PubMed: 17381335]
3. Pillai RS, Bhattacharyya SN, Filipowicz W. Repression of protein synthesis by miRNAs: how many mechanisms? Trends Cell Biol. 2007; 17:118–126. [PubMed: 17197185]
4. Liu H, Kohane IS. Tissue and process specific microRNA-mRNA co-expression in mammalian development and malignancy. PLoS ONE. 2009; 4:e5436. [PubMed: 19415117]
5. Vasudevan S, Tong Y, Steitz JA. Switching from repression to activation: microRNAs can up-regulate translation. Science. 2007; 318:1931–1934. [PubMed: 18048652]
6. Alvarez-Garcia I, Miska EA. MicroRNA functions in animal development and human disease. Development. 2005; 132:4653–4662. [PubMed: 16224045]
7. O'Rourke JR, Swanson MS, Harfe BD. MicroRNAs in mammalian development and tumorigenesis. Birth Defects Res C Embryo Today. 2006; 78:172–179. [PubMed: 16847882]
8. Meola N, Gennarino VA, Banfi S. microRNAs and genetic diseases. Pathogenetics. 2009; 2:7. [PubMed: 19889204]

9. Dressler GR. The cellular basis of kidney development. Annu Rev Cell Dev Biol. 2006; 22:509–529. [PubMed: 16822174]
10. Gao X, Chen X, Taglienti M, et al. Angioblast-mesenchyme induction of early kidney development is mediated by Wt1 and Vegfa. Development. 2005; 132:5437–5449. [PubMed: 16291795]
11. Levinson RS, Batourina E, Choi C, et al. Foxd1-dependent signals control cellularity in the renal capsule, a structure required for normal renal development. Development. 2005; 132:529–539. [PubMed: 15634693]
12. Mendelsohn C, Batourina E, Fung S, et al. Stromal cells mediate retinoid-dependent functions essential for renal development. Development. 1999; 126:1139–1148. [PubMed: 10021334]
13. Batourina E, Gim S, Bello N, et al. Vitamin A controls epithelial/mesenchymal interactions through Ret expression. Nat Genet. 2001; 27:74–78. [PubMed: 11138002]
14. Hatini V, Huh SO, Herzlinger D, et al. Essential role of stromal mesenchyme in kidney morphogenesis revealed by targeted disruption of Winged Helix transcription factor BF-2. Genes Dev. 1996; 10:1467–1478. [PubMed: 8666231]
15. Quaggin SE, Schwartz L, Cui S, et al. The basic-helix-loop-helix protein pod1 is critically important for kidney and lung organogenesis. Development. 1999; 126:5771–5783. [PubMed: 10572052]
16. Cui S, Schwartz L, Quaggin SE. Pod1 is required in stromal cells for glomerulogenesis. Dev Dyn. 2003; 226:512–522. [PubMed: 12619136]
17. Costantini F. Renal branching morphogenesis: concepts, questions, and recent advances. Differentiation. 2006; 74:402–421. [PubMed: 16916378]
18. Kobayashi A, Valerius MT, Mugford JW, et al. Six2 defines and regulates a multipotent self-renewing nephron progenitor population throughout mammalian kidney development. Cell Stem Cell. 2008; 3:169–181. [PubMed: 18682239]
19. Carroll TJ, Park JS, Hayashi S, et al. Wnt9b plays a central role in the regulation of mesenchymal to epithelial transitions underlying organogenesis of the mammalian urogenital system. Dev Cell. 2005; 9:283–292. [PubMed: 16054034]
20. Self M, Lagutin OV, Bowling B, et al. Six2 is required for suppression of nephrogenesis and progenitor renewal in the developing kidney. EMBOJ. 2006; 25:5214–5228.
21. Keller G, Zimmer G, Mall G, et al. Nephron number in patients with primary hypertension. N Engl J Med. 2003; 348:101–108. [PubMed: 12519920]
22. Luyckx VA, Brenner BM. Low birth weight, nephron number, and kidney disease. Kidney Int Suppl. 2005; 97:S68–S77. [PubMed: 16014104]
23. Saal S, Harvey SJ. MicroRNAs and the kidney: coming of age. Curr Opin Nephrol Hypertens. 2009; 18:317–323. [PubMed: 19424061]
24. Kato M, Arce L, Natarajan R. MicroRNAs and their role in progressive kidney diseases. Clin J Am Soc Nephrol. 2009; 4:1255–1266. [PubMed: 19581401]
25. Wessely O, Agrawal R, Tran U. microRNAs in kidney development: lessons from the frog. RNA Biol. 2010; 7:296–299. [PubMed: 20458188]
26. Ho J, Ng KH, Rosen S, et al. Podocyte-specific loss of functional microRNAs leads to rapid glomerular and tubular injury. J Am Soc Nephrol. 2008; 19:2069–2075. [PubMed: 18832437]
27. Harvey SJ, Jarad G, Cunningham J, et al. Podocyte-specific deletion of dicer alters cytoskeletal dynamics and causes glomerular disease. J Am Soc Nephrol. 2008; 19:2150–2158. [PubMed: 18776121]
28. Shi S, Yu L, Chiu C, et al. Podocyte-selective deletion of dicer induces proteinuria and glomerulosclerosis. J Am Soc Nephrol. 2008; 19:2159–2169. [PubMed: 18776119]
29. Sequeira-Lopez ML, Weatherford ET, Borges GR, et al. The MicroRNA-processing enzyme Dicer maintains juxtaglomerular cells. J Am Soc Nephrol. 2010; 21:460–467. [PubMed: 20056748]
30. Pastorelli LM, Wells S, Fray M, et al. Genetic analyses reveal a requirement for Dicer1 in the mouse urogenital tract. Mamm Genome. 2009; 20:140–151. [PubMed: 19169742]

31. Agrawal R, Tran U, Wessely O. The miR-30 miRNA family regulates Xenopus pronephros development and targets the transcription factor Xlim1/Lhx1. Development. 2009; 136:3927–3936. [PubMed: 19906860]
32. Zambrowicz BP, Imamoto A, Fiering S, et al. Disruption of overlapping transcripts in the ROSA beta geo 26 gene trap strain leads to widespread expression of beta-galactosidase in mouse embryos and hematopoietic cells. Proc Natl Acad Sci USA. 1997; 94:3789–3794. [PubMed: 9108056]
33. Yu J, Carroll TJ, McMahon AP. Sonic hedgehog regulates proliferation and differentiation of mesenchymal cells in the mouse metanephric kidney. Development. 2002; 129:5301–5312. [PubMed: 12399320]
34. Zhao H, Kegg H, Grady S, et al. Role of fibroblast growth factor receptors 1 and 2 in the ureteric bud. Dev Biol. 2004; 276:403–415. [PubMed: 15581874]
35. Majumdar A, Vainio S, Kispert A, et al. Wnt11 and Ret/Gdnf pathways cooperate in regulating ureteric branching during metanephric kidney development. Development. 2003; 130:3175–3185. [PubMed: 12783789]
36. Patel V, Li L, Cobo-Stark P, et al. Acute kidney injury and aberrant planar cell polarity induce cyst formation in mice lacking renal cilia. Hum Mol Genet. 2008; 17:1578–1590. [PubMed: 18263895]
37. Nadasdy T, Laszik Z, Lajoie G, et al. Proliferative activity of cyst epithelium in human renal cystic diseases. J Am Soc Nephrol. 1995; 5:1462–1468. [PubMed: 7703384]
38. Masyuk T, Masyuk A, LaRusso N. Cholangiociliopathies: genetics, molecular mechanisms and potential therapies. Curr Opin Gastroenterol. 2009; 25:265–271. [PubMed: 19349863]
39. Zhou J. Polycystins and primary cilia: primers for cell cycle progression. Annu Rev Physiol. 2009; 71:83–113. [PubMed: 19572811]
40. Edelstein CL. What is the role of tubular epithelial cell apoptosis in polycystic kidney disease (PKD)? Cell Cycle. 2005; 4:1550–1554. [PubMed: 16258272]
41. Zhou XJ, Kukes G. Pathogenesis of autosomal dominant polycystic kidney disease: role of apoptosis. Diagn Mol Pathol. 1998; 7:65–68. [PubMed: 9785003]
42. Park EY, Sung YH, Yang MH, et al. Cyst formation in kidney via B-Raf signaling in the PKD2 transgenic mice. J Biol Chem. 2009; 284:7214–7222. [PubMed: 19098310]
43. Quinlan RJ, Tobin JL, Beales PL. Modeling ciliopathies: primary cilia in development and disease. Curr Top Dev Biol. 2008; 84:249–310. [PubMed: 19186246]
44. Hoy WE, Bertram JF, Denton RD, et al. Nephron number, glomerular volume, renal disease and hypertension. Curr Opin Nephrol Hypertens. 2008; 17:258–265. [PubMed: 18408476]
45. Oxburgh L, Chu GC, Michael SK, et al. TGFbeta superfamily signals are required for morphogenesis of the kidney mesenchyme progenitor population. Development. 2004; 131:4593–4605. [PubMed: 15342483]
46. Blank U, Brown A, Adams DC, et al. BMP7 promotes proliferation of nephron progenitor cells via a JNK-dependent mechanism. Development. 2009; 136:3557–3566. [PubMed: 19793891]
47. Fogelgren B, Yang S, Sharp IC, et al. Deficiency in Six2 during prenatal development is associated with reduced nephron number, chronic renal failure, and hypertension in Br/+ adult mice. Am J Physiol Renal Physiol. 2009; 296:F1166–F1178. [PubMed: 19193724]
48. Ma W, Lozanoff S. External craniofacial features, body size, and renal morphology in prenatal brachyrrhine mice. Teratology. 1993; 47:321–332. [PubMed: 8322226]
49. Harris KS, Zhang Z, McManus MT, et al. Dicer function is essential for lung epithelium morphogenesis. Proc Natl Acad Sci USA. 2006; 103:2208–2213. [PubMed: 16452165]
50. Pazour GJ, Dickert BL, Vucica Y, et al. Chlamydomonas IFT88 and its mouse homologue, polycystic kidney disease gene tg737, are required for assembly of cilia and flagella. J Cell Biol. 2000; 151:709–718. [PubMed: 11062270]
51. Moyer JH, Lee-Tischler MJ, Kwon HY, et al. Candidate gene associated with a mutation causing recessive polycystic kidney disease in mice. Science. 1994; 264:1329–1333. [PubMed: 8191288]
52. Murcia NS, Richards WG, Yoder BK, et al. The Oak Ridge Polycystic Kidney (orpk) disease gene is required for left-right axis determination. Development. 2000; 127:2347–2355. [PubMed: 10804177]

53. Yoder BK, Tousson A, Millican L, et al. Polaris, a protein disrupted in orpk mutant mice, is required for assembly of renal cilium. Am J Physiol Renal Physiol. 2002; 282:F541–F552. [PubMed: 11832437]
54. Pan J, Snell W. The primary cilium: keeper of the key to cell division. Cell. 2007; 129:1255–1257. [PubMed: 17604715]
55. Baek D, Villen J, Shin C, et al. The impact of microRNAs on protein output. Nature. 2008; 455:64–71. [PubMed: 18668037]
56. Selbach M, Schwanhausser B, Thierfelder N, et al. Widespread changes in protein synthesis induced by microRNAs. Nature. 2008; 455:58–63. [PubMed: 18668040]
57. Lim LP, Lau NC, Garrett-Engele P, et al. Microarray analysis shows that some microRNAs downregulate large numbers of target mRNAs. Nature. 2005; 433:769–773. [PubMed: 15685193]
58. Harfe BD, McManus MT, Mansfield JH, et al. The RNaseIII enzyme Dicer is required for morphogenesis but not patterning of the vertebrate limb. Proc Natl Acad Sci USA. 2005; 102:10898–10903. [PubMed: 16040801]
59. Hayashi S, Lewis P, Pevny L, et al. Efficient gene modulation in mouse epiblast using a Sox2Cre transgenic mouse strain. Gene Expr Patterns. 2002; 2:93–97. [PubMed: 12617844]
60. Yu J, Carroll TJ, Rajagopal J, et al. A Wnt7b-dependent pathway regulates the orientation of epithelial cell division and establishes the cortico-medullary axis of the mammalian kidney. Development. 2009; 136:161–171. [PubMed: 19060336]
61. Mokrzan EM, Lewis JS, Mykytyn K. Differences in renal tubule primary cilia length in a mouse model of Bardet-Biedl syndrome. Nephron Exp Nephrol. 2007; 106:e88–e96. [PubMed: 17519557]

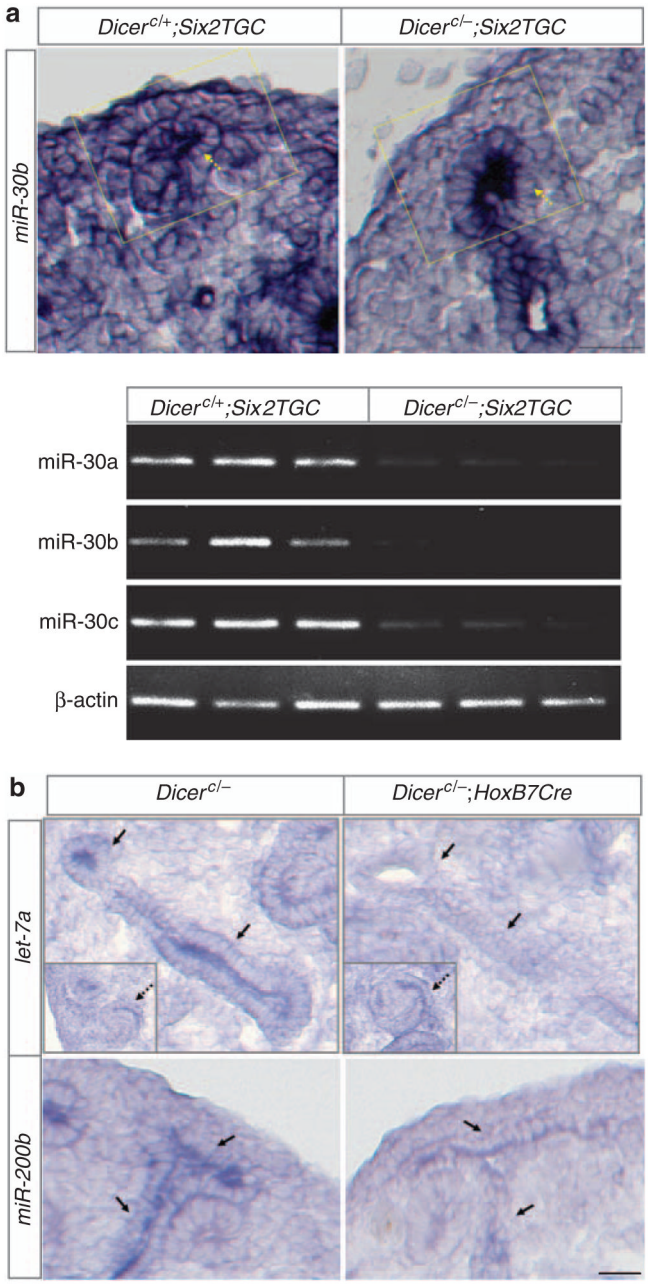

Figure 1. MicroRNA (miRNA) biogenesis is disrupted from *Dicer* depletion

In situ hybridization for miRNAs with locked nucleic acid (LNA) probes on E14.5 kidney sections and semiquantitative miRNA reverse transcription-PCR (RT-PCR) analysis on the cap mesenchyme. (**a**) miR-30b expression in the nephron progenitors (the cap mesenchyme cells overlying the ureteric tip in the boxed area) is markedly reduced to background levels in Dicer nephron mutants. Its expression in the ureteric bud epithelium (dashed arrows) is unaffected. Semiquantitative RT-PCR for miR-30a, miR-30b, miR-30c, and β-actin (control) in the fluorescence-activated cell sorting (FACS)-sorted green fluorescent protein (GFP)-positive cap mesenchyme (nephron progenitors) from three controls and three mutants showing the reduction of mature miRNAs in the E13.5 Dicer nephron mutant cap mesenchyme. The trace amount of mature miRNAs in the mutants may be due to incomplete

degradation of mature miRNAs previously produced in a subset of cap mesenchyme cells because of more mosaic expression of *Six2TGC* at earlier developmental stages (Kobayashi *et al*.[18] and unpublished observations, JY). (**b**) let-7a and miR-200b expression is greatly reduced in the ureteric bud (UB) epithelium (solid arrows) in Dicer UB mutants but unaffected in non-UB cell types (S-shaped bodies, insets and dashed arrows). Scale bars = 20 μm.

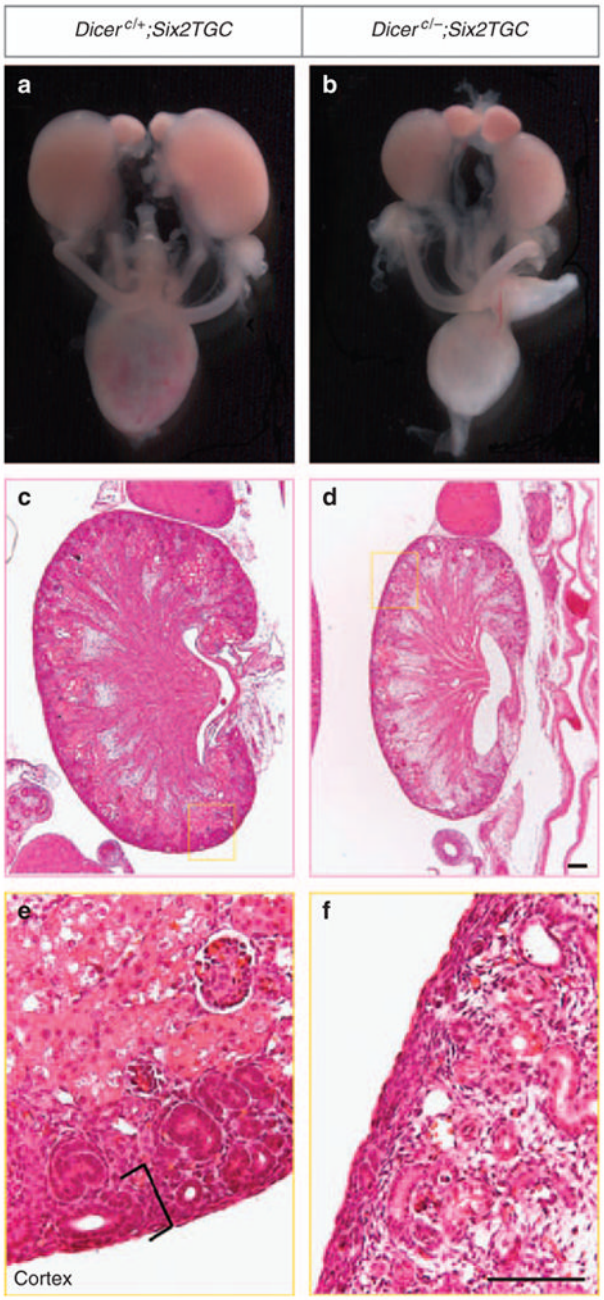

Figure 2. Disruption of *Dicer* functions from the nephron lineage leads to premature termination of nephrogenesis

(**a**, **b**) The *Dicer* nephron mutant kidneys are smaller than their control littermates at P0. (**c**–**f**) Hematoxylin and eosin staining of P0 kidney sections showing regions with a marked absence of the nephrogenic zone (brackets in **e**) except for the nephrogenic zone intersitium in the mutant kidney. Scale bars = 200 μm.

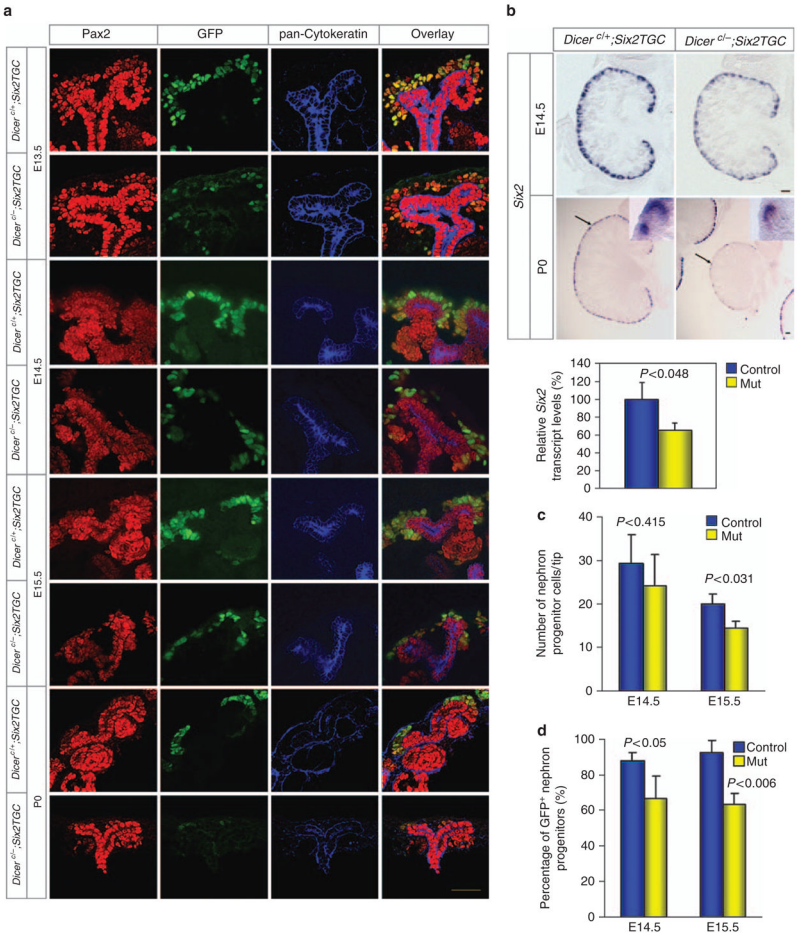

Figure 3. Reduction in the number of nephron progenitor cells and *Six2* expression resulted from *Dicer* abrogation from the nephron lineage

(**a**) Immunofluorescent staining of Pax2 to label the nephron progenitors and of green fluorescent protein (GFP). Pax2 also labels the ureteric bud (UB) epithelium and the developing nephron epithelium. The UB epithelium is demarcated with pan-Cytokeratin immunostaining. The nephron progenitors are discerned from the nephron epithelium by their positions relative to the UB epithelium. Nephron progenitors overlie the UB epithelium, whereas the nephron epithelium lies underneath the UB epithelium. All nephron progenitor cells are GFP+ in control kidneys, but a subset of them exhibit reduced or undetectable levels of GFP expression in mutants starting at E13.5. Scale bars = 50 μm. (**b**) *In situ* hybridization and quantitative reverse transcription PCR (qRT-PCR) analyses for *Six2* expression in the nephron progenitors on kidney sections. At E14.5, *Six2* expression is weaker in mutants than in controls. At P0, *Six2* transcripts are detected throughout the entire periphery of the control kidney, but are missing in most regions of the mutant kidney periphery and expressed at lower levels where detected. Arrows point to the regions enlarged in the insets. Scale bars = 100 μm. At E13.5, the *Six2* mRNA levels are 66.4% of that of controls ($n = 3$). (**c**) The number of nephron progenitor cells (Pax2+ cap mesenchyme) per ureteric tip per kidney section is not statistically significantly different between *Dicer* mutants and controls at E14.5, but decreases statistically significantly in the mutants at E15.5. (**d**) The percentage of GFP+ nephron progenitor cells (GFP+/Pax2+) is significantly reduced in *Dicer* mutants at both E14.5 and E15.5. Controls in **b**–**d**, $Dicer^{c/+}$; *Six2TGC* mice.

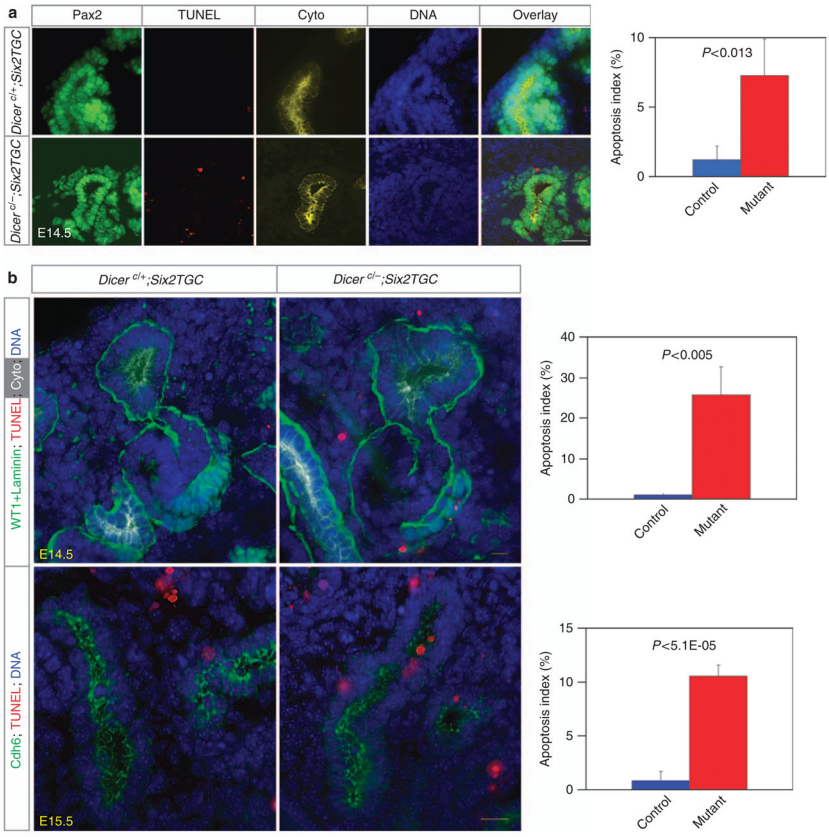

Figure 4. Elevated apoptosis in *Dicer* nephron mutant nephron progenitors (a) and nephron epithelium (b)

Immunofluorescent staining of Pax2 for nephron progenitors, the ureteric bud (UB) epithelium and part of the nephron epithelium, Laminin (basal lamina) for the nephron and UB epithelia, pan-Cytokeratin for the UB epithelium, WT1 (nuclear) for the proximal segment of the S-shaped body, and Cadherin 6 (Cdh6) for the loop of Henle. Scale bar = 20 μm.

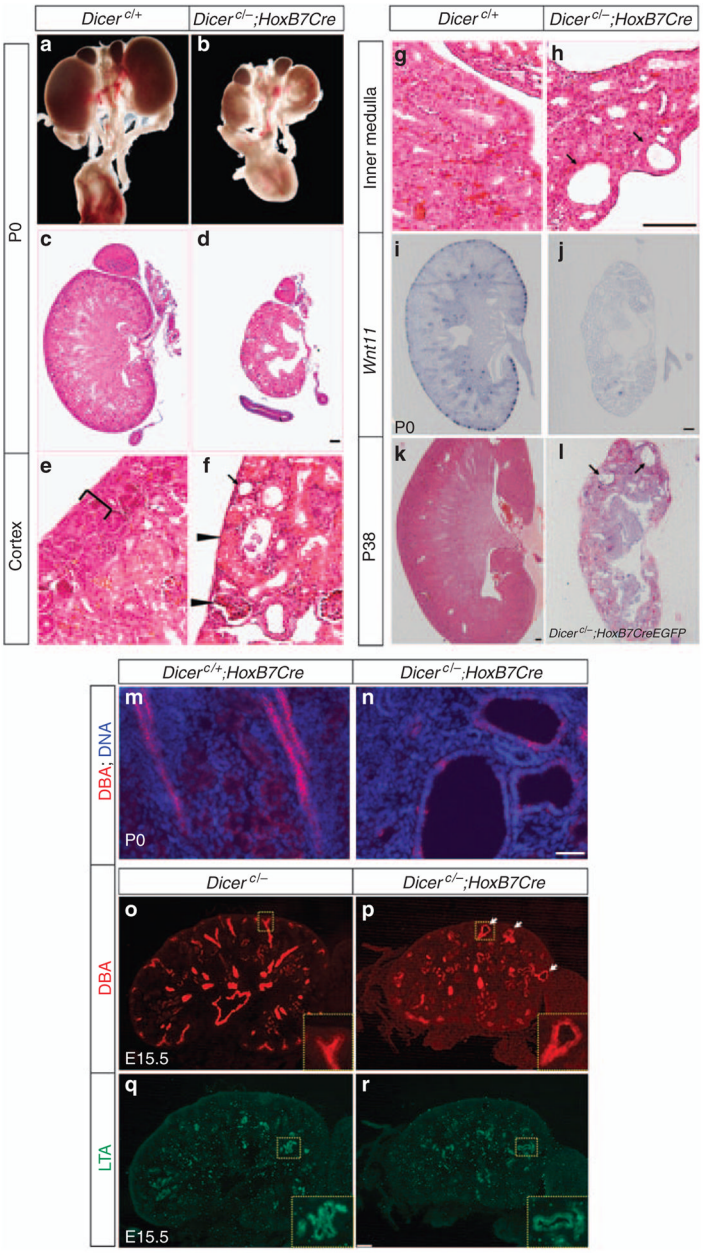

Figure 5. *Dicer* ureteric bud (UB) mutant kidneys are hypoplastic, dysplastic, and cystic

(**a**, **b**) The newborn (P0) *Dicer* UB mutant kidneys (**b**) are smaller than their wild-type littermate controls (**a**). (**c**–**h**) Hematoxylin and eosin staining of kidney sections from newborn control (**c**, **e**, **g**) and *Dicer* UB mutant (**d**, **f**, **h**) mice as indicated. The mutant renal cortex (**f**) is devoid of the nephrogenic zone (bracket in **e**) and mature nephron tubules and renal corpuscles (arrowheads) reach the kidney surface. Cysts were seen in cortical and medullary collecting ducts (arrows in **f** and **h**). (**i**, **j**) *Wnt11* mRNA expression in newborn control (**i**) and *Dicer* UB mutant (**j**) kidneys. (**k**, **l**) Hematoxylin and eosin staining of kidney sections from *Dicer*$^{c/-}$*; HoxB7CreEGFP* and control P38 kidneys. The mutant kidney is highly cystic (arrows). Scale bars = 200 μm. (**m**–**r**) Renal cysts of the UB epithelium origin in *Dicer* UB mutants. (**m**, **n**) Immunofluorescent staining of P0 kidney sections with *Dolichos bifloris* agglutinin (DBA) for the UB epithelium and Hoechst 33324 for DNA

showing cystic dilations in the UB epithelium. Scale bar = 20 μm. (**o**–**r**) Immunofluorescent staining of E15.5 kidney sections with DBA (**o**, **p**) and *Lotus tetragonolobus* agglutinin (LTA) for the proximal tubules (**q**, **r**). Cystic dilations were observed in the UB epithelium but not the proximal tubules. Scale bar = 100 μm.

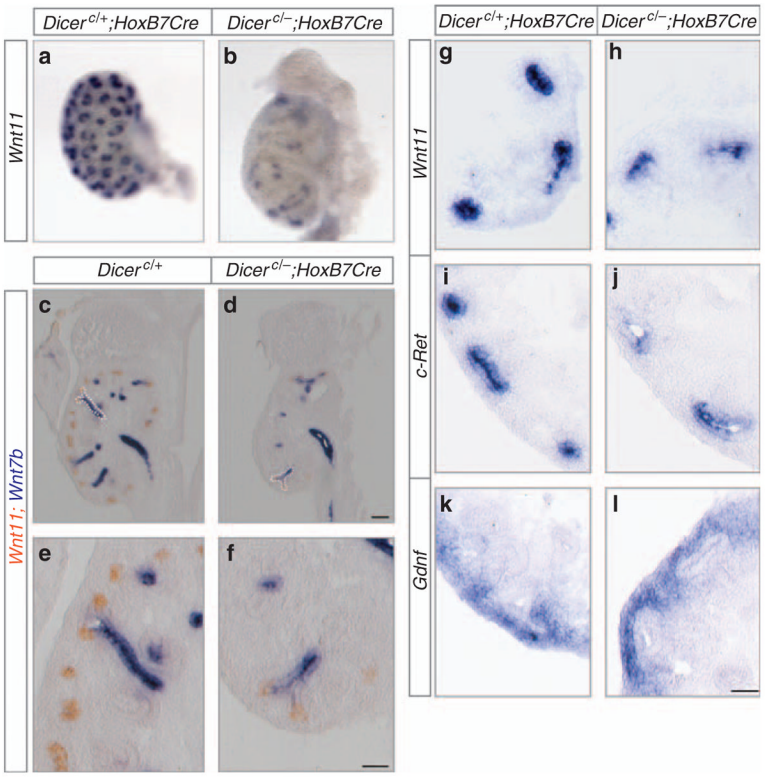

Figure 6. Disrupted branching morphogenesis of the *Dicer* ureteric bud (UB) mutant kidneys at E13.5

(**a**, **b**) Whole-mount *in situ* hybridization analysis demonstrating a significant loss of *Wnt11* expression in *Dicer* UB mutant kidneys (**b**) compared with their control littermates (**a**). (**c**–**f**) Representative images of double *in situ* hybridization on kidney sections showing that in mutants (**d**, **f**), all the *Wnt7b*-positive UB trunks bear *Wnt11*-positive branching tips, but the expression levels of *Wnt11* are significantly reduced compared with their control littermates (**c**, **e**). (**g**–**l**) *In situ* hybridization on kidney sections reveals a significant reduction in the levels of expression of *Wnt11* and *c-Ret* in the branching UB tips of mutants compared with their control littermates. No detectable reduction in *Gdnf* signals in the mesenchyme was observed in the mutants compared with the control littermates. Scale bars = 50 μm.

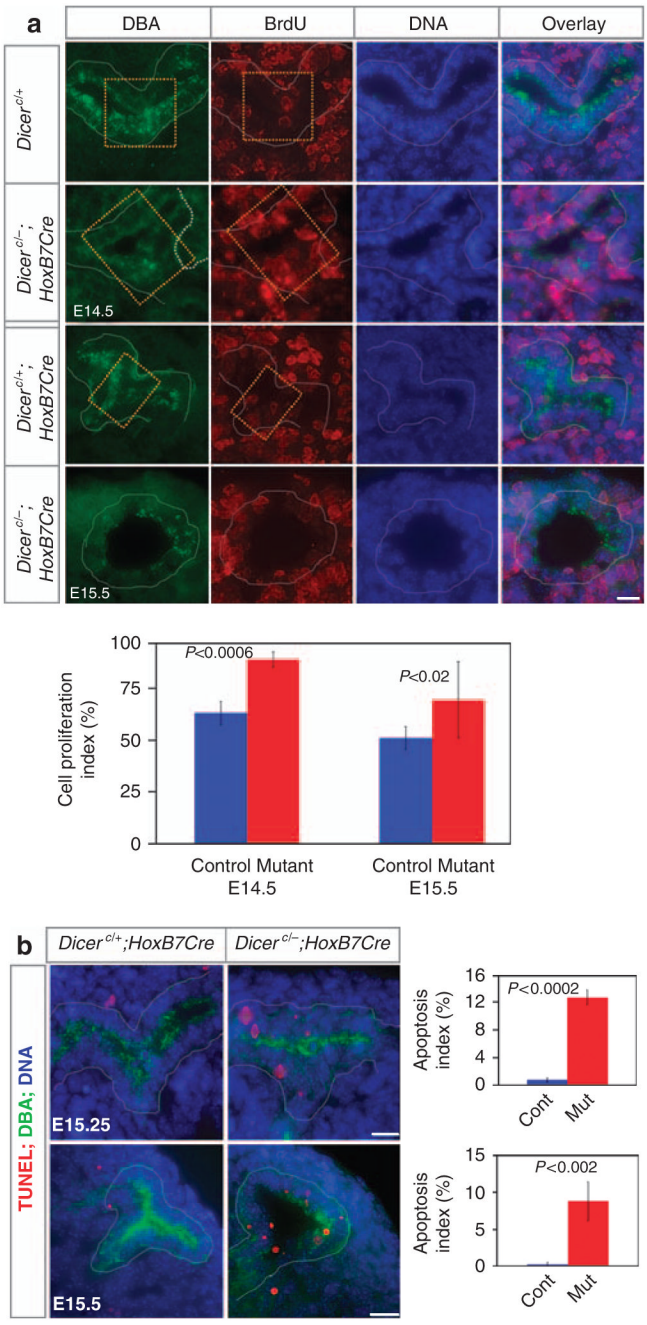

Figure 7. Cell proliferation and cell death prior to and following the onset of cyst formation

(**a**) Increased cell proliferation precedes and follows the onset of cyst formation in the nascent ureteric bud (UB) trunk region of *Dicer* mutants. Cell proliferation was analyzed in the yellow boxed areas and the entire cysts (outlined with white dashed lines) at E14.5 and E15.5 with 5-bromodeoxyuridine (BrdU) labeling. BrdU incorporation into dividing cells was visualized with anti-BrdU antibodies (red). *Dolichos biflorus* agglutinin (DBA) staining (green) delineates the UB epithelium. A significant increase in the cell proliferation rates was observed in the *Dicer* UB mutants ($n = 4$) in the cystic UB epithelium at E15.5 ($P<0.02$) as well as in the nascent trunk region at E14.5 ($P<0.0006$) when compared with their control littermates ($n = 4$). (**b**) Increased apoptosis in UBs of *Dicer* UB mutants. The cell death rate

was measured with TdT-mediated dUTP nick end labeling (TUNEL) analysis (red) in the UB epithelium stained with DBA (green). A significant increase in cell death was observed in both non-cystic (n = 3) and cystic UBs (n = 4) relative to their control littermates (n = 4) at E15.25 and E15.5, respectively. Cont, control; Mut, mutant. Scale bars = 15 μm.

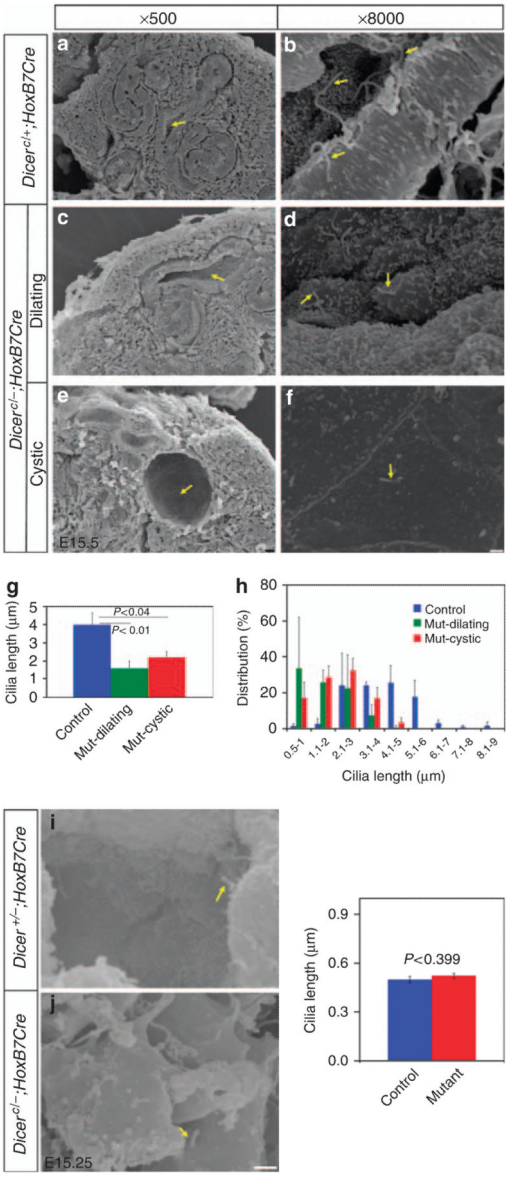

Figure 8. Reduction in the length of the primary cilium from deletion of *Dicer* from the ureteric bud (UB) epithelium

(**a**–**f**) Scanning electron microscopic images of primary cilia (arrows in **b**, **d**, and **f**) in the UB epithelium at E15.5. Panels **b**, **d**, and **f** are higher magnification images of the regions indicated by arrows in panels **a**, **c**, and **e,** respectively. Mutant cilia were shorter than controls and most of them were reduced to short stubs. Scale bar = 10 μm for panels **a**, **c,** and **e** and 1 μm for panels **b**, **d**, and **f**. (**g**) Control primary cilia averaged 4.01±0.66 μm (n = 124) in length, whereas mutant cilia averaged 1.60±0.40 μm in the dilating UBs (n = 100; P<0.01) and 2.21±0.31 μm in the cystic UBs (n = 189; P<0.04). No statistically significant differences were observed in cilia length between dilating and cystic UBs (P<0.29). (**h**) Distribution of primary cilia length in control and dilating and cystic mutant UB epithelia. (**i**, **j**) Scanning electron micrographs showing short primary cilia at E15.25 (arrows in **i** and **j**) in the non-dilating UB epithelium and no significant differences in the length of the primary cilium between the controls (**i**) and mutants (**j**). Scale bar = 1 μm.

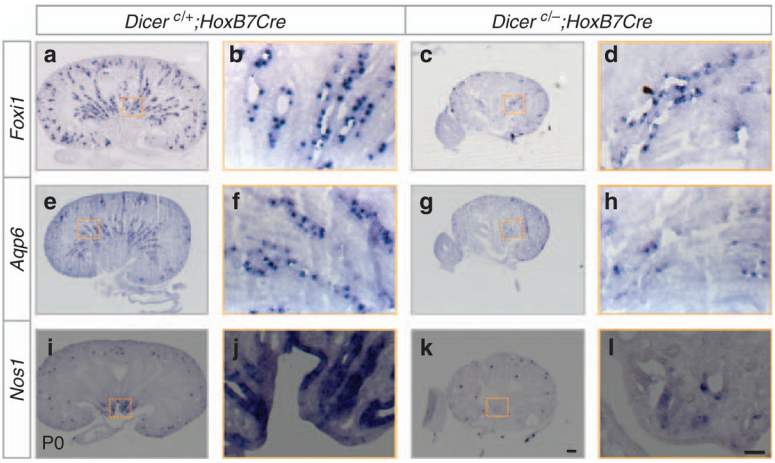

Figure 9. Terminal differentiation of the collecting duct is affected in *Dicer* ureteric bud (UB) mutants

In situ hybridization analysis of expression of markers for terminal differentiation of collecting duct cells on P0 kidney sections. *Foxi1* expression is similar in *Dicer* mutants and controls. *Aqp6* and *Nos1* are expressed at reduced levels and less frequently in the mutant collecting ducts. Scale bars = 200 μm for panels **a**, **c**, **e**, **g**, **i**, and **k**, and 50 μm for panels **b**, **d**, **f**, **h**, **j**, and **l**.